Point defect determination by photoluminescence and capacitance–voltage characterization in a GaN terahertz Gunn diode*

Li Liang(李 亮)†, Yang Lin-An(杨林安), Zhou Xiao-Wei(周小伟), Zhang Jin-Cheng(张进成), and Hao Yue(郝 跃)

School of Microelectronics, Key Laboratory of Wide Bandgap Semiconductor Materials and Devices of Ministry of Education, Xidian University, Xi'an 710071, *China*

(Received 23 November 2012; revised manuscript received 29 December 2012)

Photoluminescence (PL) measurement is used to study the point defect distribution in a GaN terahertz Gunn diode, which is able to the degrade high-field transport characteristic during further device operation. PL, secondary ion mass spectroscopy (SIMS), transmission electron microscope (TEM), and capacitance–voltage (C–V) measurements are used to discuss the origin of point defects responsible for the yellow luminescence in structures. The point defect densities of about 10^{11} cm^{-2} in structures are extracted by analysis of C–V characterization. After thermal annealing treatment, diminishments of point defect densities in structures are efficiently demonstrated by PL and C–V results.

Keywords: GaN terahertz Gunn diode, point defect, photoluminescence, capacitance–voltage

PACS: 71.55.Eq, 72.10.Fk, 73.61.Ey **DOI:** 10.1088/1674-1056/22/8/087104

1. Introduction

The gallium nitride (GaN) based Gunn diode is one of promising candidates in terahertz source technology because of its high frequency and high output power.[1,2] In recent years, numerous researches have reported that the charge trapping effect introduced by deep-level crystal defects in GaN brings on evident degradation in negative-differential-resistance (NDR) characteristic of GaN high-field transport, thereby leading to significant decreases of radio frequency power and conversion efficiency in terahertz device operation.[3,4] Up to now, there has been only one report on the actual fabrication of a GaN-based Gunn diode with a 5-μm long transit region,[5] which, however, did not show a stable oscillation similar to that of a GaAs Gunn diode, although it had been predicted that a GaN Gunn diode with at least 1-μm long or shorter transit region could generate an oscillation frequency of over 200 GHz. Obviously, the requirement for high-quality GaN Gunn diode is still limited by the inconvenient crystal defects because of immature GaN crystal growth nowadays. Therefore, the crystal defects in the actual GaN terahertz Gunn diodes need an in-depth and systemic investigation.

Generally, the point defect is an important component in GaN crystal defects. It was reported that point defects, particularly, the deep acceptors, trap charges to form charge-centers.[6] Their behaviors act as scattering centers and increase the scattering probability when the electron domain forms and propagates through the transit region of the Gunn diode, which, therefore, deteriorates the device characteristics. The point defect distribution can be efficiently detected and identified by the analysis of photoluminescence (PL) spectra, where the yellow luminescence (YL) emission is an important defect-related deep-level phenomenon in GaN. Xu *et al.*[7] reported that gallium vacancy ($V_{\rm Ga}$)-involved defects are the origin responsible for the YL emission in unintentional-doped GaN. Xu *et al.*[8] indicated that carbon-involved defects are originally responsible for the YL emission in non-polar and semipolar GaN. As is well known, the capacitance–voltage ($C-V$) measurement is widely used to characterize the trap centers in epitaxy. Xie *et al.*[9] demonstrated that the $V_{\rm Ga}$-related defects in (Al)GaN bulk layers are responsible for the frequency-dependent capacitance dispersion in pinch-off region, where the trap density about 10^{12} cm^{-2}·eV^{-1} is present. Lü *et al.*[10] reported that point defects such as $V_{\rm Ga}$-related defects induced by irradiation on GaN can be detected by C–V measurement. Wang *et al.*[11] suggested that the trap in the surface of the ungated region between source and drain can be analyzed by the frequency dispersion characteristics of GaN HEMT. Chu *et al.*[12] showed that AlGaN/GaN interface trap states are responsible for the trapping behavior in 10 kHz–1 MHz frequency ranges, and trap density of 10^{13} cm^{-2}·eV^{-1}–10^{14} cm^{-2}·eV^{-1} is obtained. Despite these outstanding results, studies on point defects of GaN Gunn diode have been sparse up to now. Therefore, a systematic analysis of PL spectrum and C–V characterization of GaN Gunn diode should be made to further seek the point defects distribution.

*Project supported by the National Natural Science Foundation of China (Grant Nos. 61076079 and 61274092), the Doctoral Program Fund of the Ministry of Education of China (Grant No. 20090203110012), and the Major Program and State Key Program of the National Natural Science Foundation of China (Grant No. 60890191).

†Corresponding author. E-mail: LL860726@163.com

© 2013 Chinese Physical Society and IOP Publishing Ltd

2. Experimental procedure

We fabricated multiple layer epitaxial samples for n^+ (200 nm)–n^- (1000 nm)–n (200 nm)–n^+ (400 nm) GaN Gunn diodes. GaN Gunn diode samples A and B with 650-nm GaN buffer layer were grown on *c*-plane sapphire substructure by using metal–organic chemical vapor deposition (MOCVD) under the approximately same growth conditions. An 80-nm thick AlN layer was grown at 960 °C as a nucleation layer. Trimethygallium and ammonia were used as source gases and hydrogen was used as a carrier gas. Disilane was introduced as an Si-doping source. In our experiment, Si-doping concentrations of n^+ layer and n^- layer were chosen to be 1×10^{18} cm^{-3} and 1×10^{17} cm^{-3}, respectively. An electron concentration of about 4×10^{16} cm^{-3} is achieved for undoped GaN material at room temperature due to the existence of impurity.[13] It is close to designed concentration of n layer. Therefore, we chose the undoped GaN as the n layer in the actual growth process. In this work, we put the emphasis on the studies of PL spectra and *C*–*V* characterization that are helpful to reveal the point defect origin and distribution in GaN Gunn diode. Secondary ion mass spectroscopy (SIMS) and transmission electron microscope (TEM) are also employed to evaluate GaN Gunn diodes.

3. Results and discussion

Figure 1 shows the PL spectra at 300 K for samples A and B. It shows that samples A and B produce different YL intensities centred at 2.2 eV–2.3 eV in the spectra. The ratio of YL intensity to band-edge emission intensity (I_{YL}/I_{BE}) is corresponding to the density of the deep-acceptor defect.[14] whose values are 5.8 and 3.2 for samples A and B, respectively. It is reported that the point defects are regarded as the candidate of the deep-acceptors to enhance the YL emission. However, the origin of the point defects resulting in YL emission is still a controversial problem. Some research groups suggested that the carbon-involved complex is responsible for YL emission,[8] and some authors regard the V_{Ga}-involved defect as the candidate of YL emission origin.[7] These possible factors that influence the intensity of YL emission in the structures are investigated.

We examine SIMS results of samples A and B, both of which are grown on *c*-plane sapphire substrate under Ga-face polar condition, so that the replacement of N by C in two samples is of the identical possibility to form site C_N.[8] Figures 2(a) and 2(b) show that samples A and B have the same carbon impurity concentration of 6×10^{16} cm^{-3}, while PL measurements indicate that the I_{YL}/I_{BE} of sample A (5.8) is almost twice that of sample B (3.2). In addition, Xu *et al.*[8] reported on the variation trend of I_{YL}/I_{BE} value with carbon impurity concentration, indicating that the I_{YL}/I_{BE} value related to carbon impurity concentration of 6×10^{16} cm^{-3} is around 0.6 in GaN material, which is much smaller than the I_{YL}/I_{BE} value in GaN Gunn diode. Therefore, we confirm that the carbon-involved complex is not the main component of point defect related to the YL emission in GaN Gunn diodes.

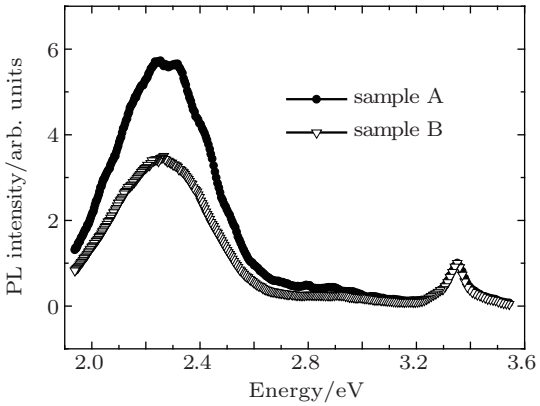


Fig. 1. Comparison of PL spectrum between samples A and B.

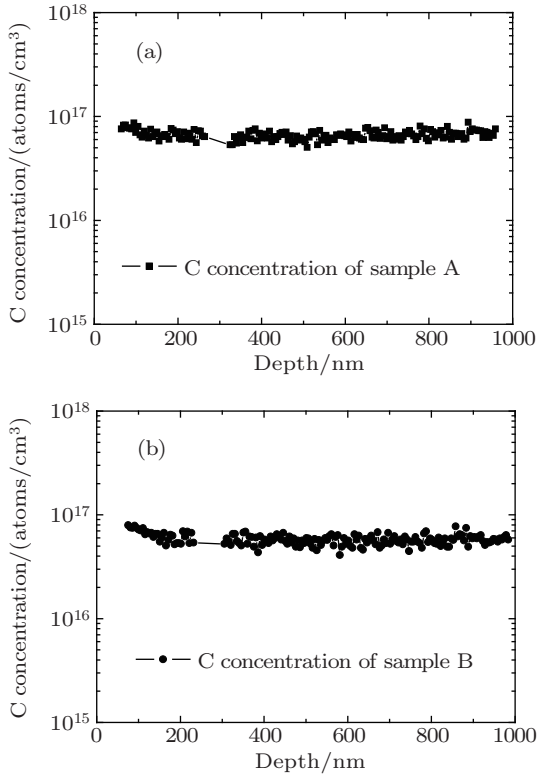


Fig. 2. Carbon concentration distributions of (a) sample A and (b) sample B.

Some studies mentioned that the edge dislocations are involved in YL emission, while other investigations indicated that the edge dislocations in GaN films are nonradiative recombination centers, which themselves cannot cause or determine YL emission originating from radiative recombination centers.[15] Recently, several reports have shown that the stress field of thread edge dislocations is likely to trap V_{Ga}-involved complex with a large binding energy in wurtzite GaN, which

can promote the formation of V_{Ga}.[16,17] From the experiment of this work, we assume that point defects resulting in YL emission mainly consist of the V_{Ga} trapped dislocations at the edge, which is introduced to interpret the discrepancy of YL emission.

Figures 3(a) and 3(b) show the diffraction vector $g = 11$–20 weak beam cross-section TEM images of samples A and B, respectively, which make visible the edge component of the dislocations.[18] In the section 1-μm thick away from the surface, the values of edge dislocation density (N_{EDs}) of samples A and B are 3.5×10^9 cm^{-2} and 2.0×10^9 cm^{-2}, respectively. According to the assumption of V_{Ga} trapped at edge dislocations, there must be a density corresponding to V_{Ga}, which is proportional to the edge dislocation density.

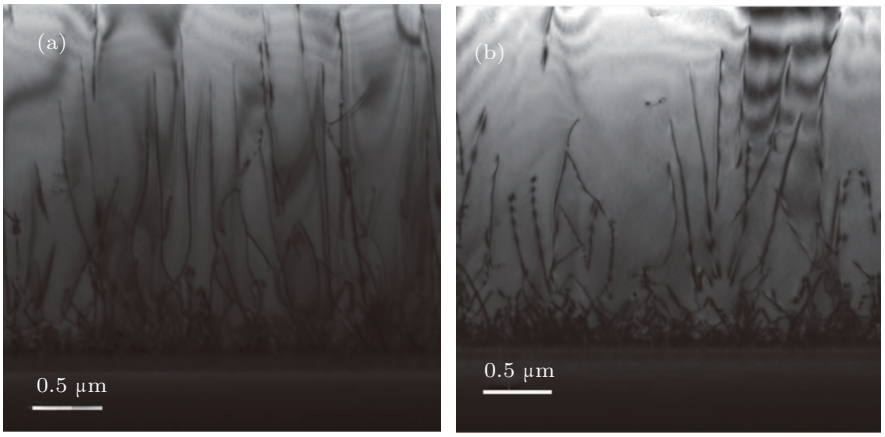


Fig. 3. Diffraction vector $g = 11$–20 weak beam cross-section TEM images of (a) sample A and (b) sample B.

To test this, C–V characterization is proposed to extract the trap density. According to the previous work,[19] an accurate capacitance C_0 is shown as follows:

$$C_0 = (\omega_1 - \omega_2)\frac{D_t}{1+D_t^2}\left[\frac{\omega_1 D_1}{C_1(1+D_1^2)} - \frac{\omega_2 D_2}{C_2(1+D_2^2)}\right], \tag{1}$$

$$D_t = \frac{\left[C_1C_2(1+D_1^2)(1+D_2^2)\right]^2}{\left[\omega_1C_2(1+D_2^2) - \omega_2C_1(1+D_1^2)\right]\left[\omega_1D_1C_2(1+D_2^2) - \omega_2D_2C_1(1+D_1^2)\right]}, \tag{2}$$

where C_1, G_1, and D_1 correspond to measure condition ω_1; C_2, G_2, and D_2 correspond to measure condition ω_2; D_t is the surface state factor. Figures 4(a) and 4(b) show the C–V curves of samples A and B measured at 100 kHz and 1 MHz, from which we deduce a corrected curve for samples A and B in order to eliminate the impact factors, respectively.

During the high frequency (100 kHz) measurement, electrons are captured by the traps such as point defects or edge dislocations, in which case the electrons cannot keep up with the change rate of high frequency, therefore, they are confined into the traps. However, it has been reported that effects of influence factors such as surface states on the capacitance distribution grow up and cause significant measurement errors with the increase of the frequency. Thus, we employ the C–V data of 100 kHz, rather than those of 1 MHz, to compare with the corrected data. Therefore, the trap density (N_{trap}) is given as follows:

$$N_{trap} = \frac{\int V\,\mathrm{d}C}{e\cdot A}, \tag{3}$$

where $\int V\,\mathrm{d}C$ is the integration of the area difference between the 100 kHz and the corrected C–V curves, e the electron charge, and A the Schottky contact area between Hg probe and material surface. According to Eq. (3), The values of N_{trap} in samples A and B are calculated to be 4.6×10^{11} cm^{-2} and 2.2×10^{11} cm^{-2}, respectively.

Table 1 shows that the difference between N_{trap} and N_{EDs} is approximately of two orders of magnitude, therefore we confirm that the edge dislocation is not the main component of the traps. Due to the fact that the N_{trap} are proportional to N_{EDs}, it reveals that the V_{Ga} at edge dislocations is the dominating component of trap. Furthermore, N_{trap} also has a variation trend similar to the I_{YL}/I_{BE}, therefore we confirm that the point defects resulting in YL emission originate from V_{Ga} at edge dislocations, and the point defect density about 10^{11} cm^{-2} is present in GaN Gunn diode.

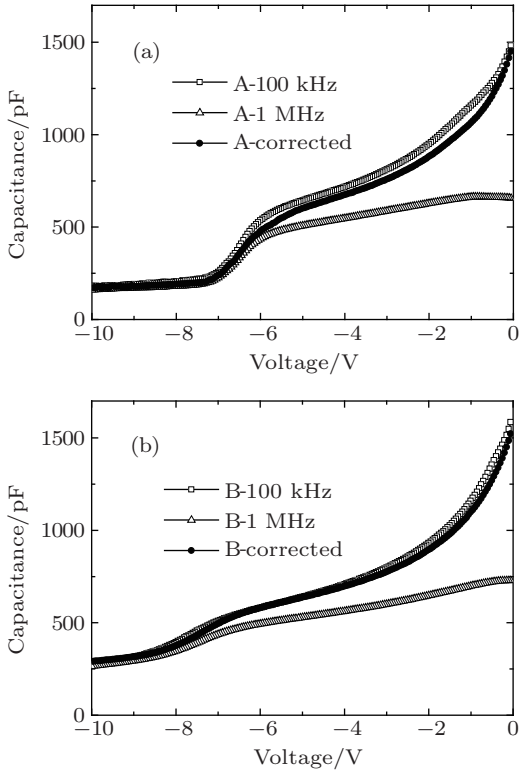


Fig. 4. Measured and corrected *C*–*V* curves of (a) sample A and (b) sample B.

Table 1. Values of I_{YL}/I_{BE}, N_{trap}, and N_{EDs} of samples A and B.

Sample	I_{YL}/I_{BE}	N_{trap}/cm^{-2}	N_{EDs}/cm^{-2}
A	5.8	4.6×10^{11}	3.5×10^{9}
B	3.2	2.2×10^{11}	2.0×10^{9}

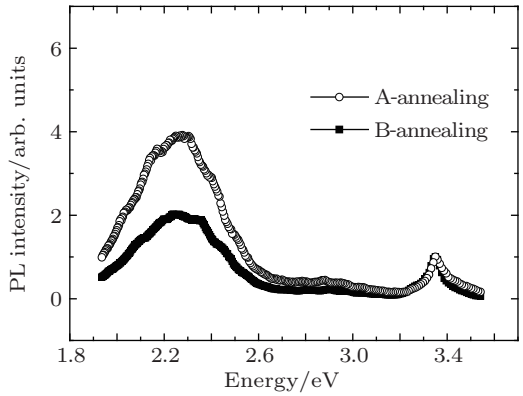


Fig. 5. Comparison of PL spectra of samples A and B after thermal annealing.

The existence of point defects in GaN Gunn diodes adversely restricts the electrical properties and degrades the quality of the fabricated device features. In order to optimize the structures, we perform thermal annealing treatment on samples A and B. Cole *et al.*[20] reported that high-temperature thermal annealing is helpful to depress the crystal defect density and improve the GaN crystal quality. Maeda *et al.*[21] demonstrated that the deep-level acceptors are efficiently annihilated through thermal annealing. Thermal annealing treatment on samples A and B at 800 °C for 1 min in the nitrogen atmosphere is performed to suppress the point defect distribution in GaN Gunn diode. Figure 5 shows the values of I_{YL}/I_{BE} of samples A (3.8) and B (2.0) after annealing. Comparing before and after annealing, it is shown that the deep-level acceptor distribution in sample A (sample B) is lowered by 34.5% (37.5%) after annealing.

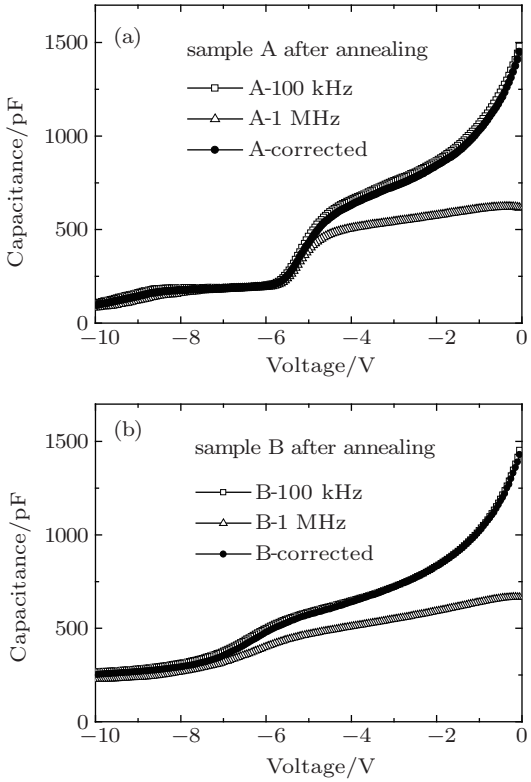


Fig. 6. Measured and corrected *C*–*V* curves of (a) sample A and (b) sample B after thermal annealing.

Figures 6(a) and 6(b) show *C*–*V* characterizations of samples A and B after annealing, from which we observe that the high frequency (100 kHz) curve is very close to the corrected *C*–*V* curve in each sample, indicating efficient diminishment of point defects in structures after annealing. The point defect densities of samples A and B are calculated to 2.4×10^{11} cm^{-2} and 1.3×10^{11} cm^{-2}, respectively. Therefore, the point defect densities of samples A and B reduce 31.4% and 35.0%, respectively, following the variations of YL emission in samples. The effect of the annealing on the carbon-involved complex distribution is still unknown. However, the carbon-involved complex itself is not the main component of point defect related to the YL emission in GaN Gunn diode. The effect of carbon-involved complex on total point defect distribution can be neglected during the annealing. Furthermore, we emphasize the characteristics of total point defect reduction due to the annealing, revealing the fact that the reduction of point defects by annealing is conducive to the improvement on the NDR characteristic in GaN terahertz Gunn diodes.

4. Conclusions

In conclusion, point defect research to analyze the charge trapping effect remains a longstanding challenge in guaranteeing the stable NDR in GaN terahertz Gunn diode. Toward this objective, we use PL, SIMS, TEM, and *C*–*V* measurements to demonstrate that the point defects are V_{Ga}-related defects trapped at edge dislocations, rather than at carbon-involved complex, which are the origin of point defects responsible for the YL emissions in structures. Furthermore, we use the *C*–*V* characterization to extract the point defect densities (about 10^{11} cm^{-2}) in structures. We employ thermal annealing to optimize structures, which reveals that the point defect densities are approximately lowered by 30% by analyses of the PL and *C*–*V* results.

References

[1] Macpherson R F, Dunn G M and Pilgrim N J 2008 *Semicond. Sci. Technol.* **23** 055005

[2] Macpherson R F and Dunn G M 2008 *Appl. Phys. Lett.* **93** 062103

[3] Yang L A, He H B, Mao W and Hao Y 2011 *Appl. Phys. Lett.* **99** 153501

[4] Bayram C, Vashaei Z and Razeghi M 2010 *Appl. Phys. Lett.* **97** 181109

[5] Yilmazoglu O, Mutamba K, Pavlidis D and Karaduman T 2008 *IEEE Trans. Electron. Dev.* **55** 6

[6] Saarinen K, Laine T, Kuisma S, Nissila J, Hautojarvi P, Dobrzynski L, Baranowski J M, Pakula K, Stepniewski R, Wojdak M, Wysmolek A, Suzuki T, Leszczynski M, Grzegory I and Porowski S 1997 *Phys. Rev. Lett.* **79** 3030

[7] Xu F J, Shen B, Lu L, Miao Z L, Song J, Yang Z J, Zhang G Y, Hao X P, Wang B Y, Shen X Q and Okumura H 2010 *J. Appl. Phys.* **107** 023528

[8] Xu S R, Hao Y, Zhang J C, Cao Y R, Zhou X W, Yang L A, Ou X X, Chen K and Mao W 2010 *J. Crystal Growth* **312** 3521

[9] Xie S Y, Yin J Y, Zhang S, Liu B, Zhou W and Feng Z H 2009 *Solid-State Electronics* **53** 1183

[10] Lü L, Zhang J C, Xue J S, Ma X H, Zhang W, Bi Z W, Zhang Y and Hao Y 2012 *Chin. Phys. B* **21** 037104

[11] Wang X H, Pang L, Chen X J, Yuan T T, Luo W J, Zheng Y K, Wei K and Liu X Y 2011 *Acta Phys. Sin.* **60** 097101 (in Chinese)

[12] Chu R M, Zhou Y G, Chen K J and Lau K M 2003 *Phys. Stat. Sol. (c)* **7** 2400

[13] Nakamura S 1991 *Jpn. J. Appl. Phys.* **30** L1705

[14] Yoshikawa M, Sugie R, Murakami M, Matsunobe T, Matsuda K and Ishida H 2006 *Appl. Phys. Lett.* **88** 161905

[15] You J H and Johnson H T 2007 *Phys. Rev. B* **76** 115336

[16] Elsner J, Jones R, Haugk M, Frauenheim Th, Heggie M I, Öberg S and Briddon P R 1998 *Phys. Rev. B* **76** 115336

[17] Du D C, Zhang J C, Ou X X, Wang H, Chen K, Xue J S, Xu S R and Hao Y 2011 *Chin. Phys. B* **20** 037805

[18] Ponce F A, Cherns D, Young W T and Steeds J W 1996 *Appl. Phys. Lett.* **69** 770

[19] Li L, Yang L A, Zhang J C, Zhang L X, Dang L S, Kuang Q W and Hao Y 2012 *Solid-State Electronics* **68** 98

[20] Cole M W, Ren F and Pearton S J 1997 *Appl. Phys. Lett.* **71** 3004

[21] Maeda N, Nozawa K, Hirayama Y and Kobayashi N 1998 *J. Crystal Growth* **190** 359